Computers and Concrete, *Vol. 20, No. 5 (2017) 545-553*
DOI: https://doi.org/10.12989/cac.2017.20.5.545

Shaking table test of pounding tuned mass damper (PTMD) on a frame structure under earthquake excitation

Wei Lin*[1], Qiuzhang Wang[1a], Jun Li[2b], Shanghong Chen[1c] and Ai Qi[1d]

[1]*School of Civil Engineering, Fuzhou University, 2 Xueyuan Road, Fuzhou, Fujian, China*
[2]*Centre for Infrastructural Monitoring and Protection, School of Civil and Mechanical Engineering, Curtin University, Kent Street, Bentley, WA 6102, Australia*

(Received July 25, 2017, Revised August 10, 2017, Accepted August 19, 2017)

Abstract. A pounding tuned mass damper (PTMD) can be considered as a passive device, which combines the merits of a traditional tuned mass damper (TMD) and a collision damper. A recent analytical study by the authors demonstrated that the PTMD base on the energy dissipation during impact is able to achieve better control effectiveness over the traditional TMD. In this paper, a PTMD prototype is manufactured and applied for seismic response reduction to examine its efficacy. A series of shaking table tests is conducted in a three-story building frame model under single-dimensional and two-dimensional broadband earthquake excitations with different excitation intensities. The ability of the PTMD to reduce the structural responses is experimentally investigated. The results show that the traditional TMD is sensitive to input excitations, while the PTMD mostly has improved control performance over the TMD to remarkably reduce both the peak and root-mean-square (RMS) structural responses under single-dimensional earthquake excitation. Unlike the TMD, the PTMD is found to have the merit of maintaining a stable performance when subjected to different earthquake loadings. In addition, it is also indicated that the performance of the PTMD can be enhanced by adjusting the initial gap value, and the control effectiveness improves with the increasing excitation intensity. Under two-dimensional earthquake inputs, the PTMD controls remain outperform the TMD controls; however, the oscillation of the added mass is observed during the test, which may induce torsional vibration modes of the structure, and hence, result in poor control performance especially after a strong earthquake period.

Keywords: vibration control; pounding tuned mass damper (PTMD); energy dissipation; frame structure; earthquake excitation

1. Introduction

With the rapid growth of economy, stricter requirement for the safety of structure has been proposed, especially under earthquake and wind-induced excitations (Lin et al. 2013, YI *et al*. 2015, Li *et al*. 2009). Due to the unpredictable characteristic of earthquake and the increasing complexity of modern structures, it is difficult to predict seismic responses of the structures (Chen *et al*. 2014, Soong and Spencer 2002, Mishra *et al.* 2013). In recent years, more and more Structural Health Monitoring (SHM) systems were incorporated in large-scale structures. The performance assessment results can guide the maintenance work and keep the structure in a relatively healthy condition. However, possible catastrophic failure may be occurred during extreme events and the safety of the structure cannot be guaranteed. The development of structural vibration control, which is generally believed to be an effective way in enhancing the safety and the applicability of structures under harmful excitations (Yi *et al.* 2013, Zhang and Ou 2017, Weber *et al.* 2016). With the comprehensive in-situ monitoring data from the SHM systems, the control approach can now be more precisely designed and it is expected to have better control effectiveness.

In general, the vibration control technology consists of passive, active, semi-active and hybrid control. Among them, the passive control technology is widely applied in the field of civil engineering owing to its low cost, little negative influence on disturbing the structural stability, and no consumption of external energy inputs. As one of the earliest passive devices, tuned mass dampers (TMDs) have gained widespread applications in many well-known structures (Soong and Spencer 2002), such as John Hancock building in Boston and Citicorp office building in New York. Unlike active and semi-active control, TMD control can be operated effectively without external energy inputs. The effectiveness of TMD on wind-induced vibration is widely recognized in academia. Kawaguchi *et al.* (1992) and Xu *et al.* (1992) validated the effectiveness of TMD for tall building under wind loads. Besides, more efforts have been devoted and the control efficacy is demonstrated by many scholars, most of which are dealing with the vibration control problems under wind load and human-induced load problem (Varadarajan and Nagarajaiah 2004, Lee *et al.* 2006, Tubino and Piccardo 2015).

∗Corresponding author, Associate Professor
E-mail: cewlin@fzu.edu.cn
[a]Master Student
[b]Senior Lecturer
[c]Associate Professor
[d]Professor

ISSN: 1598-8198 (Print), 1598-818X (Online)

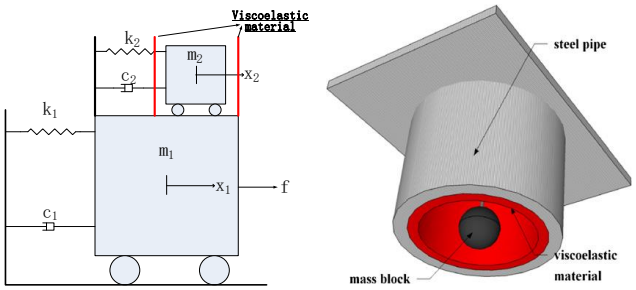

(a) Schematic model (b) PTMD prototype

Fig. 1 Schematic model and prototype of PTMD

Despite the effectiveness of TMDs, there are some deficiencies in its application. In general, a massive mass is required to ensure the efficacy of the TMD in the design, which may cause the construction difficulty in its implement on large-scale structures. Furthermore, the control effectiveness of TMDs is found to be very sensitive to the tuned frequency and even the dominant frequency of excitation (Nagarajaiah 2009, Casado *et al*. 2007, Occhiuzzi *et al*. 2008, Weber and Feltrin 2010). In addition, the effectiveness of TMDs on earthquake vibration control has been controversial. Early in 1994, researchers have pointed out that a single TMD has limit control effectiveness under earthquake excitation (Xu *et al*. 2017), and it may even increase the structural responses. Vilaverde *et al*. (1994 and 1995) investigated the effectiveness of a TMD in three different structures, including a frame structure, a shear wall structure and a suspension bridge. Their numerical and experimental results showed inconsistent control results for different structures under different seismic inputs. It has also been indicated in other researches that one single TMD cannot guarantee the control performance during earthquake excitations (Xiang and Nishitani 2014, Lin *et al*. 2015).

Accordingly, in order to overcome the shortcomings of single TMD, multiple TMDs have been proposed by tuning them to target at different frequencies for a broadband control, or hybrid control combining TMD with active or semi-active devices has been implemented. Inaudi and Kelly (1995) proposed a TMD control system added with a nonlinear hysteretic damper, which acts as the role of energy dissipation. This TMD system was applied in Taipei 101 building and validated to be more efficient than the traditional TMD with a given frequency band. The advantages of active or semi-active devices have also been incorporated with TMDs to improve control results. Active springs and semi-active stiffness mechanism have been adopted to adaptively change the frequency of TMDs. (Ricciardelli *et al*. 2000, Varadarajan and Nagarajaiah 2004, Eason 2013). Although the active or semi-active devices may guarantee a better and more stable performance, additional sensors and higher cost are needed during operation. Another improved control passive device, Pounding Tuned Mass Damper (PTMD), was proposed by Song *et al*. (2016), based on the fact that a large amount of energy can be dissipated through pounding. Zhang *et al*. (2012) analyzed the control performance of the PTMD in a power transmission tower subjected to earthquake excitation, and verified its superiority over the conventional TMD. A PTMD prototype was then manufactured and applied to vibration control of a pipeline (Song *et al*. 2016).

Table 1 Optimized parameters of modified pounding model

Parameters	β_1	ξ_2	s_1	s_2
value	10560	0.8	1.3	1.1

In the previous study, the first author of this paper (Lin *et al.* 2017) designed a PTMD for the Canton Tower based on dynamic characteristic derived from the in-situ monitoring data. The simulation results proved that the PTMD has a relatively stable control performance, and the improvement over the traditional TMD is obvious, especially when severe earthquake excitation was considered. Later, to further enhance the applicability of the control devices in large-scale structures, an improved control scheme with multiple PTMD were proposed (Lin *et al.* 2016), better control effectiveness were realized and fewer installation cost is required.

This paper extends the writer's pervious numerical studies and seeks for experimentally verification of the ability of the PTMD in reducing structural responses over a wide range of loading conditions. Shaking table tests are designed and conducted on the uncontrolled, TMD and PTMD controlled systems excited with various seismic loadings. Both the peak and the RMS responses of the structural mode are compared for evaluating the superiority of the PTMD over the TMD. Also, the improvement of the control effectiveness related to the excitation intensity, as well as the influence of initial gap in the PTMD is discussed according to the experimental results.

2. Modeling of PTMD controlled system

TMD absorbs the vibration energy through the movement of the attached mass, while PTMD sets an additional collar to dissipate more vibration energy from impact. A schematic model of a PTMD is shown in Fig. 1. A viscoelastic layer to the limitation collar set around the attached mass. When the attached mass hit the layer during its movements, the vibration energy can be further dissipated through the deformation of viscoelastic layer, and the viscoelastic layer is able to recover after each collision. As a result, during operation, this device can absorb vibration energy of the host structure and transfer it to the kinetic energy and potential energy of the attached mass, as well as some heat energy from the impact.

Assume an n degree-of-freedoms' structure installed with a single PTMD at the n^{th} degree of freedom (DOF), then the equation of motion can be expressed as

$$\boldsymbol{M}\ddot{\boldsymbol{X}}+\boldsymbol{C}\dot{\boldsymbol{X}}+\boldsymbol{K}\boldsymbol{X}=\boldsymbol{E}\boldsymbol{F}+\boldsymbol{D}\boldsymbol{P} \tag{1}$$

where $\boldsymbol{M}$, $\boldsymbol{C}$, $\boldsymbol{K}$ are the mass, damping, and stiffness matrices of the coupled system, which has n+1 DOFs; $\boldsymbol{F}$ is the excitation force, and during earthquake excitation

$$\boldsymbol{F}=-\boldsymbol{M}\ddot{x}_g(t) \tag{2}$$

where $\ddot{x}_g(t)$ is the acceleration time history record during an earthquake. $\boldsymbol{P}$ is the control force acting between the

added mass and the host structure; matrices $\boldsymbol{E}$ and $\boldsymbol{D}$ are the index matrix indicating the DOFs of the excitation and the control forces, respectively.

$$\begin{bmatrix} m_1 & & & \\ & \ddots & & \\ & & m_n & \\ & & & m_r \end{bmatrix}\begin{bmatrix} \ddot{x}_1 \\ \vdots \\ \ddot{x}_n \\ \ddot{x}_r \end{bmatrix}+\begin{bmatrix} c_1 & \cdots & c_{1n} & 0 \\ \vdots & \ddots & \vdots & \vdots \\ c_{n1} & \cdots & c_n+c_r & -c_r \\ 0 & \cdots & -c_r & c_r \end{bmatrix}\begin{bmatrix} \dot{x}_1 \\ \vdots \\ \dot{x}_n \\ \dot{x}_r \end{bmatrix} +\begin{bmatrix} k_1 & \cdots & k_{1n} & 0 \\ \vdots & \ddots & \vdots & \vdots \\ k_{n1} & \cdots & k_n+k_r & -k_r \\ 0 & \cdots & -k_r & k_r \end{bmatrix}\begin{bmatrix} x_1 \\ \vdots \\ x_n \\ x_r \end{bmatrix}=\begin{bmatrix} f_1 \\ \vdots \\ f_n \\ f_r \end{bmatrix}+\begin{bmatrix} 0 \\ \vdots \\ p \\ -p \end{bmatrix} \tag{3}$$

where m_r represents the mass of the PTMD, c_r and k_r are respectively the connecting damping and stiffness of the PTMD, and p is the pounding force between the attached mass and the viscoelastic layer. Extracting the last line in Eq. (3), the equation of motion referring to the dynamic response of PTMD mass is expressed as

$$m_r\ddot{x}_r - c_r\dot{x}_n + c_r\dot{x}_r - k_r x_n + k_r x_r = f_r - p \tag{4}$$

then the governing equation of the added mass as

$$m_r\ddot{x}_r + c_r\dot{x}_r + k_r x_r = k_r x_n + c_r\dot{x}_n + f_r - p \tag{5}$$

Assemble those terms related to the host structure, the governing equation is expressed as

$$\begin{bmatrix} \boldsymbol{M}_n & 0 \end{bmatrix}\begin{bmatrix} \ddot{\boldsymbol{X}}_n \\ \ddot{x}_r \end{bmatrix}+\left(\begin{bmatrix} \boldsymbol{C}_n & 0 \end{bmatrix}+\begin{bmatrix} 0 & \cdots & 0 & 0 \\ \vdots & \ddots & \vdots & \vdots \\ 0 & \cdots & c_r & -c_r \end{bmatrix}\right)\begin{bmatrix} \dot{\boldsymbol{X}}_n \\ \dot{x}_r \end{bmatrix}+ \left(\begin{bmatrix} \boldsymbol{K}_n & 0 \end{bmatrix}+\begin{bmatrix} 0 & \cdots & 0 & 0 \\ \vdots & \ddots & \vdots & \vdots \\ 0 & \cdots & k_r & -k_r \end{bmatrix}\right)\begin{bmatrix} \boldsymbol{X}_n \\ x_r \end{bmatrix}=\boldsymbol{F}+\begin{bmatrix} 0 \\ p \end{bmatrix} \tag{6}$$

where $\boldsymbol{K}_n$, $\boldsymbol{M}_n$ and $\boldsymbol{C}_n$ respectively represent the stiffness, mass and damping matrixes of the host structure. Reconstruction of the above equation yields

$$\boldsymbol{M}_n\ddot{\boldsymbol{X}}_n+\boldsymbol{C}_n\dot{\boldsymbol{X}}_n+\boldsymbol{K}_n\boldsymbol{X}_n=\boldsymbol{F}+\boldsymbol{C}_d\begin{bmatrix} \dot{\boldsymbol{X}}_n \\ \dot{x}_r \end{bmatrix}+\boldsymbol{K}_d\begin{bmatrix} \boldsymbol{X}_n \\ x_r \end{bmatrix}+\begin{bmatrix} 0 \\ p \end{bmatrix} \tag{7}$$

where

$$\boldsymbol{C}_d=\begin{bmatrix} 0 & \cdots & 0 & 0 \\ \vdots & \ddots & \vdots & \vdots \\ 0 & \cdots & c_r & -c_r \end{bmatrix},\boldsymbol{K}_d=\begin{bmatrix} 0 & \cdots & 0 & 0 \\ \vdots & \ddots & \vdots & \vdots \\ 0 & \cdots & k_r & -k_r \end{bmatrix} \tag{8}$$

By comparing with uncontrolled equation of motion, the control force F_{PTMD} acting on the host structure can be decoupled and extracted as

$$\boldsymbol{F}_{PTMD}=\boldsymbol{C}_d\begin{bmatrix} \dot{\boldsymbol{X}}_n \\ \dot{x}_r \end{bmatrix}+\boldsymbol{K}_d\begin{bmatrix} \boldsymbol{X}_n \\ x_r \end{bmatrix}+\begin{bmatrix} 0 \\ p \end{bmatrix} \tag{9}$$

It is clear from Eq. (9) that the damping force is composed of three terms, which are related to the damping, the stiffness and the impact, respectively. During operation, the impact will happen between the mass and the viscoelastic layer. In the previous study, the first author of this paper proposed an improved pounding force model which is validated by impact tests (Lin *et al.* 2016). It is assumed that during the approaching period, the impact

Table 2 Natural frequencies of the frame model (unit: Hz)

Mode	1	2	3	4	5
Frequency	1.12	1.33	2.34	2.64	3.12

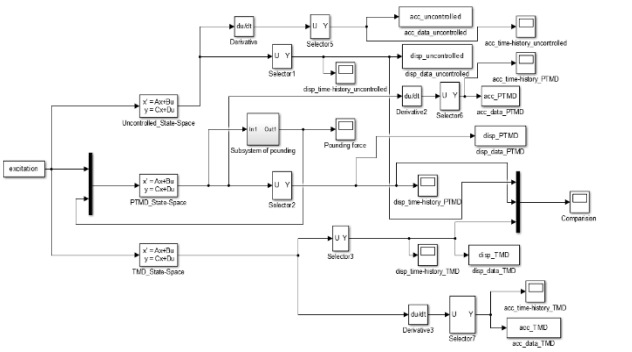

Fig. 2 Simulink diagram

damping, c, is not only affected by the stiffness, but also influenced by the different extent of compressed area which can be considered as a function of the approaching velocity, denoted as

$$\bar{c}(t)=2\bar{\xi}_1\sqrt{\bar{\beta}\sqrt{\delta(t)}\frac{m_1m_2}{m_1+m_2}}+\bar{\xi}_2\dot{\delta}(t)^{s_2} \tag{10}$$

in which $\bar{\xi}_1$ is the damping ratio correlated with the coefficient of restitution, and $\bar{\xi}_2$ is the damping ratio correlated with approaching velocity.

$$\begin{aligned} p(t)&=\bar{\beta}\delta^{s_1}(t)+\bar{c}(t)\dot{\delta}(t) \quad &\left(\dot{\delta}(t)>0\right)\\ p(t)&=\bar{\beta}\delta^{s_1}(t) \quad &\left(\dot{\delta}(t)<0\right)\end{aligned} \tag{11}$$

$\bar{\beta},\bar{\xi}_2,s_1,s_2$ are parameters to be decided in this model. During application, these parameters are relevant to the characteristic of the viscoelastic material. For the particular VE layers selected in this paper, the optimized parameters are tuned as shown in Table 1 (Lin *et al.* 2016).

3. Trial simulation with simulink

A simple simulation is conducted on a standard 10-story frame structure to provide a design reference for the following experiment. The first five natural frequencies of the model are shown in Table 2. The first mode is the bending mode along the long-axis of the structure with the natural frequency of 1.12 Hz.

A PTMD is assumed to be connected on top of the frame and the mass ratio between the added mass and the host structure is 0.02. The frequencies of the TMD and the PTMD are tuned as the same as the first natural frequency of the host structure. A Simulink block shown in Fig. 2 is established based on the state equations derived from the equations of motion of the controlled system, referred to Eq. (1) to Eq. (8). Fig. 3 and Table 3 briefly show that better control effectiveness can be provided by the PTMD compared to the traditional TMD, the improvement of the

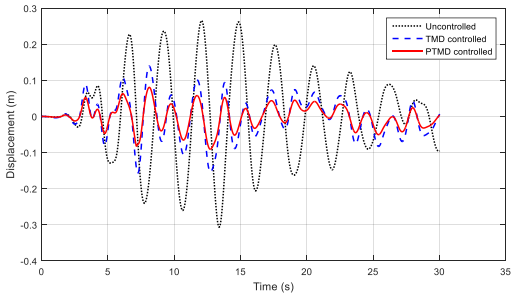

(a) 0.1 g

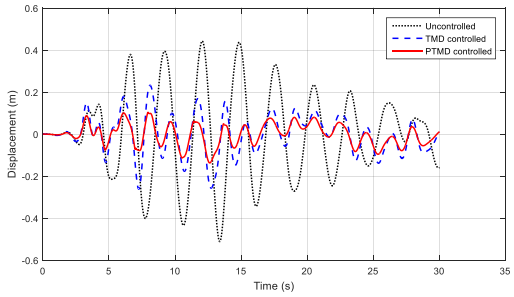

(b) 0.2 g

Fig. 3 Comparison of the responses under El Centro excitation (gap: 0.15 m)

Table 3 Comparison of structural responses subjected to earthquake loadings

Excitation			Uncontrolled	TMD	PTMD gap (m)			
					0.1	0.15	0.2	0.25
El Centro	0.1 g	Peak	0.307	0.179	0.104	0.122	0.132	0.178
		RMS	0.125	0.050	0.042	0.046	0.048	0.050
	0.2 g	Peak	0.511	0.298	0.133	0.130	0.136	0.214
		RMS	0.209	0.083	0.056	0.056	0.059	0.079
	0.3 g	Peak	0.716	0.417	0.177	0.172	0.179	0.201
		RMS	0.292	0.116	0.070	0.072	0.075	0.089
Wenchuan	0.1 g	Peak	0.220	0.221	0.134	0.109	0.123	0.190
		RMS	0.088	0.077	0.038	0.036	0.042	0.068
	0.2 g	Peak	0.367	0.368	0.144	0.118	0.131	0.201
		RMS	0.147	0.128	0.049	0.047	0.048	0.067
	0.3 g	Peak	0.514	0.516	0.188	0.130	0.142	0.206
		RMS	0.206	0.179	0.051	0.051	0.057	0.68

control effectiveness has a lot do to with the initial gap value and the excitation intensity. And the results also indicate that the PTMD tends to have better control effectiveness under more severe earthquake. Therefore, in the following designed experiment, the performance of PTMD under various excitations will be verified, and the influence of the initial gap value will be analyzed through the experiment.

4. Experimental setup

Fig. 4 shows a three-story building installed with a PTMD on the top. To simulate a high-rise building, the

Fig. 4 Shaking table test of the experimental model

building model is designed with low stiffness. It has a plane dimension of 1.2 m×0.9 m, and the height of each story is 0.9 m. The beams in the building model have a cross section of 38 mm×25 mm and the columns have a cross section of 48 mm×35 mm. The beams and the columns are rigidly connected, and the bottoms of the columns are rigidly connected to the shaking table. After setting up the model, additional masses were placed on each floor to achieve the measured natural frequency of 1.3 Hz. In the following section, the direction *x* and *y* will refer to the long and the short axis of the model.

Fig. 5 shows a single PTMD installed in the building model for experiments. The PTMD has an attached mass of 10 kg. The mass ratio between the attached mass and the host structure is around 0.02. The connection hinge on the top of the device guarantees that the PTMD can move in all directions. The connection rod has a length of 40 cm, which results in the same frequency of the PTMD as the host structure. A limitation collar is installed around the attached mass, and a 6 mm thick viscoelastic material is attached to the inner wall of the collar, which absorbs vibrational energy during collision between the attached mass and the collar. The viscoelastic material is tested in the previous study (Zhang *et al*. 2012). Without the limitation collar, the experimental setup is used for the TMD controlled cases. It is found from the numerical study that the initial gap significantly affects the control performance. Accordingly, two types of collar are designed. As shown in Figure 5, the small collar is used to constrain the displacement of the rod (Gap 1), while the large one restricts the displacement of the mass block (Gap 2).

Both sinusoidal and earthquake excitations are adopted to excite the building model. El Centro (NS 1940) and Wenchuan (NS 2012) earthquake records are selected with a peak acceleration set between 0.1 g and 0.2 g. Both single-dimensional and two-dimensional earthquake excitations are considered in different cases. Under the single-dimensional earthquake, it is assumed that the excitation is only acted along the long-axis direction (*x*-direction) of the building model. The two-dimensional earthquake refers to the vibration components along the long-axis and the short-axis directions (*x*- and *y*-direction) are taken into account simultaneously. For each excitation case, uncontrolled,

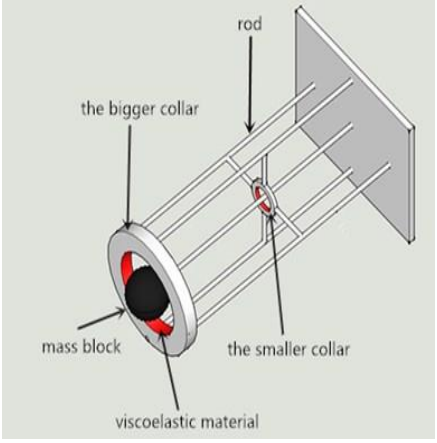

(a) Sketch of PTMD

(b) PTMD in the experiment

Fig. 5 Installation of PTMD

TMD controlled and PTMD controlled scenarios are examined, and the structural responses are measured and compared.

5. Shaking table test results

5.1 Single-dimensional excitation results

In the following simulation, the control effectiveness η was defined to as a metric to evaluate the control performance of the damper. The control effectiveness is expressed as

$$\eta = \frac{R_u - R_c}{R_u} \times 100\% \tag{12}$$

where R_u and R_c refer to the uncontrolled and controlled responses, respectively.

Sinusoidal excitation along x direction is first adopted to excite the structure, the frequency is set as 1.3 Hz, which is close to the first natural frequency of the structure. The amplitudes of the excitation are set as 0.1 g. Fig. 6 compares the uncontrolled and controlled acceleration responses on top of the frame structure. One can see that from the results, both TMD and PTMD controls can produce over 50% reduction on acceleration response, while

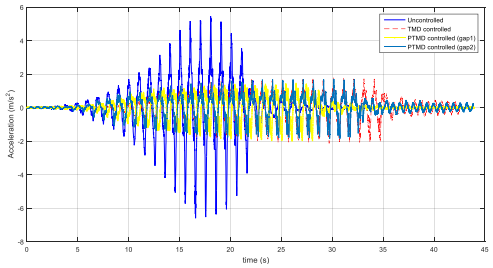

(a) comparison of controlled and uncontrolled acceleration responses

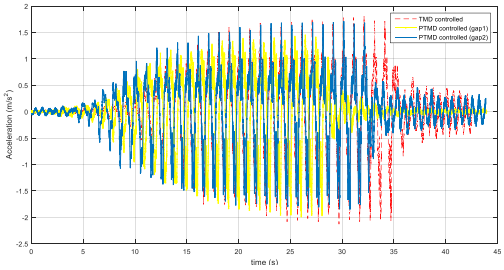

(b) comparison of TMD and PTMD controlled acceleration responses

Fig. 6 Time-history of acceleration responses under sinusoidal excitation

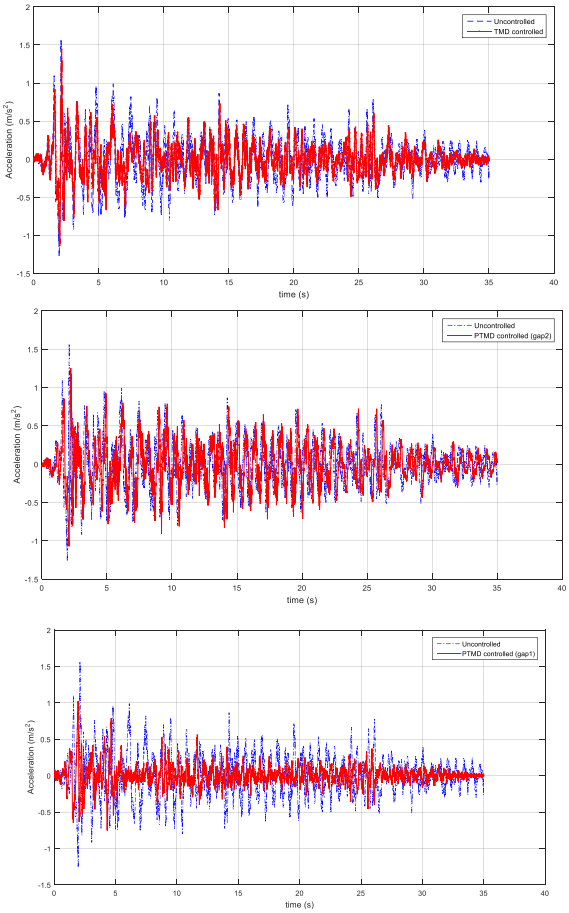

Fig. 7 comparison of the acceleration responses under El Centro earthquake excitation (0.1 g)

PTMD control has slight improvement compared to TMD control. In this case, it seems that the gap value has little

Table 4 Control effectiveness of the acceleration responses subjected to El Centro earthquake excitation

Excitation	Value	Uncontrol	TMD		PTMD (Gap1)		PTMD (Gap2)	
			Acc (m/s^2)	η	Acc (m/s^2)	η	Acc (m/s^2)	η
El Centro (0.1 g)	Peak	1.56	1.44	7.5%	0.76	51.5%	1.25	19.8%
	RMS	0.29	0.28	5.1%	0.09	70.3%	0.22	23.7%
El Centro (0.2 g)	Peak	2.43	2.08	14.5%	1.37	43.9%	1.79	26.6%
	RMS	0.44	0.33	25.4%	0.13	71.5%	0.13	70.1%

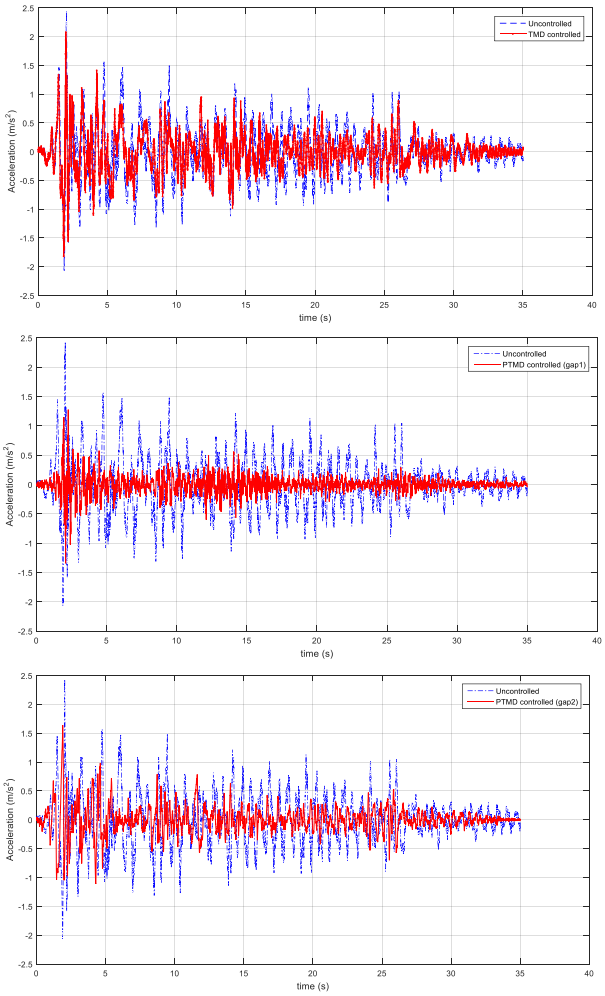

Fig. 8 Comparison of the acceleration responses under El Centro earthquake excitation (0.2 g)

influence on the control effectiveness.

Fig. 7 shows the control results when earthquake strikes, the acceleration responses on top of the frame are compared. It is obvious that TMD control can hardly reduce the seismic responses. When excessive gap value is selected (referred as Gap 2 case in the figure), only slight reduction ratio is obtained since the impact between the mass and the limitation can hardly occur, and only small amount of energy is dissipated through pounding. As it is shown in the last plot of Fig. 7, when the initial gap reduces, the PTMD begin to dissipate more energy and then the acceleration responses can be greatly reduced.

Fig. 8 shows the acceleration results when the excitation intensity grows to 0.2 g. Compared to the 0.1 g cases, it is observed during the vibration test that the pendulum mass moves more rapidly and hit the VE layer more frequently with larger velocities. Table 4 further compares the peak and the RMS control effectiveness. The control results show that the TMD can have some control ratio on the RMS responses in this excitation case, but it barely has control effect for the peak acceleration responses. On the contrary, both PTMD cases can now produce impressive control results on both the peak and the RMS responses. It seems that with the increase of the excitation intensity, the impact between the mass and the VE layer becomes easier and the pounding is more severe. Which will result in larger deformation of the VE layer and more vibration energy be dissipated during the impact. Therefore, comparing to 0.1 g excitation case, even relatively larger initial gap value (Gap2 case) can now generate much better control effectiveness. As the excitation intensity increased from 0.1 g to 0.2 g, the control effectiveness of the peak acceleration is increased by 6.8%, while the improvement of the control effectiveness of the RMS responses is remarkable. However, no improvement is found for the peak and RMS control effectiveness for Gap1 case. The control effectiveness of the peak responses is even reduced by almost 8%. These results suggest that the optimal selection of the initial value has a lot to do with the excitation intensity.

Another strong ground motion, Wenchuan earthquake record whose frequency components are quite different from El Centro Wave, is further adopted to verify the control effectiveness of the PTMD under broadband tests. Fig. 9 and Table 5 shows the comparison of uncontrolled and controlled acceleration responses under different excitation intensities. Poor performances of TMD are observed, rather than reducing the responses, even larger response is obtained at higher excitation intensity. All these results presented show that all of the PTMD control systems perform significantly better than the TMD systems. In the low amplitude tests, PTMD with Gap 1 achieves a 56.1% and 78.3% reductions in the peak and RMS acceleration. The reductions of PTMD with Gap 2 are 33.8% and 63.7%, respectively. Although the performance is no better than the Gap 1 case, the reduction is also very impressive. In the high amplitude tests, both PTMDs have better control results, especially for the peak responses reductions. Gap 1 and Gap 2 cases improve the control effectiveness of the peak responses by 7.2% and 20.9%. Gap 2's improvement is more obviously with the growing excitation. The improvement results indicate that during Wenchuan earthquake inputs, the initial value may be exceeded the optimal values for the Gap 2 case. And Gap 1 may be close to the optimal selection of the initial gap value. The comparison of the control effectiveness under two excitation intensities indicate that little improvement may be achieved if further reducing the initial gap. It is mentioned that a PTMD can dissipate the vibration energy of the host structure through the movement of the mass, the impact between the mass and the VE layer, and the deformation of the VE layer. If the gap continues to reduce, the vibration amplitude of the mass will be limit, which means few Kinect energy will be dissipated. Moreover, if too small the gap is, the relative velocity between the mass

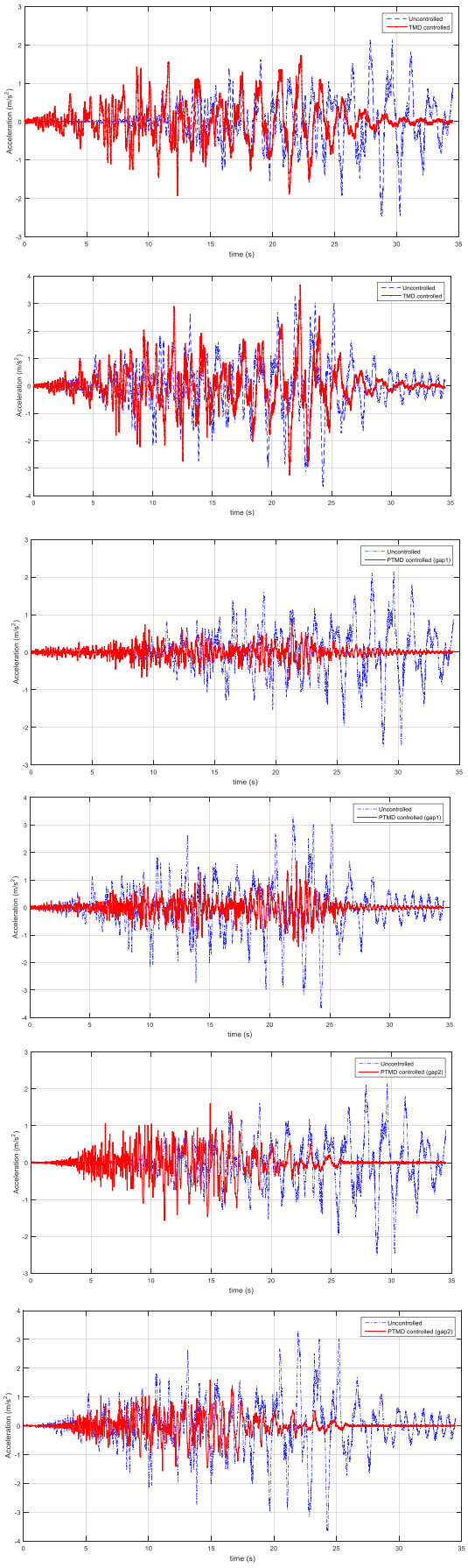

Fig. 9 Comparison of the acceleration responses under Wenchuan earthquake excitation (0.1 g: left vs. 0.2 g: right)

Table 5 Control effectiveness of the acceleration responses subjected to Wenchuan earthquake excitation

Excitation intensity	Value	Uncontrol	TMD		PTMD (Gap1)		PTMD (Gap2)	
			Acc (m/s^2)	η	Acc (m/s^2)	η	Acc (m/s^2)	η
Wenchuan (0.1 g)	Peak	2.50	1.93	22.9%	1.10	56.1%	1.66	33.8%
	RMS	0.58	0.49	15.0%	0.13	78.3%	0.21	63.7%
Wenchuan (0.2 g)	Peak	3.66	3.67	-0.3%	1.35	63.3%	1.66	54.7%
	RMS	0.86	0.75	12.8%	0.19	78.5%	0.21	75.8%

and the VE layer will be small, and then the severity of the impact will be limit as well.

5.2 Two-dimensional excitation results

The designed universal hinge connection guarantees that the PTMD can move in any horizontal directions. More test with the earthquake inputs are from the x- and y- directions simultaneously to verify the performance of the PTMD under multi-dimensional excitation. It is assumed that in the following session, the ratio of the *x* to *y* peak ground motions is 1:0.85. Comparisons of the control results of the uncontrolled, TMD and PTMD controlled systems are listed in Table 6, and particularly Fig. 4 presents the time-history acceleration responses along the *x*- and *y*- directions when subjected to Wenchuan earthquake with the earthquake intensity of the *x*-direction and the *y*-direction to be set as 0.2 g and 0.17 g, respectively.

The PTMD was shown to have better reduction on both the peak and the RMS responses in most cases. However, unstable performance is observed for PTMDs, and the control results are not as good as those under one-dimensional inputs. One can see that from the table, under El Centro excitation, at low excitation tests, the PTMDs present poor control effectiveness, especially along the *x*-direction. As the peak intensity of the ground motion grows to 0.2 g, the peak responses are significantly reduced, but the reduction on the RMS responses along the *x*-direction is little, only 0.8% and 24.5% in Gap 1 and Gap 2 cases. It is worth mentioned that the reductions on the *y*-direction is more obvious than the *x*-direction for both PTMD cases. As from the table, PTMDs (Gap1) is able to produced 45.5% and 36.1% reduction on the peak and the RMS responses. Under Wenchuan earthquake, the TMD hardly has control effectiveness, the oscillation of the mass seems to enlarge the acceleration of the host structure. In PTMD controlled system, the dampers can reduce the peak and the RMS responses. The control effectiveness is better for the Gap 1 PTMD than the Gap 2 PTMD at low excitation intensity. While similar control results are obtained during high intensity earthquake inputs. If further examining the time-history curves during the two-dimensional tests, one is able to see that there are undesirable oscillations after the strongest parts of the ground motion. It is also observed from the tests that the PTMDs have a spiral swing during two-dimensional inputs, which makes the PTMD cannot hit the VE layer positively. Worse situation happens when somehow the spiral swing induced the torsional vibration of the host structure. The problem indicates that to use one

Table 6 Control effectiveness under multi-dimensional earthquake

Excitation	Value	Uncontrolled	TMD		PTMD (Gap1)		PTMD (Gap2)	
			Acc (m/s^2)	η	Acc (m/s^2)	η	Acc (m/s^2)	η
El Centro (0.1 g)	Peak(x)	1.36	1.29	5.8%	1.12	17.9%	1.36	0.1%
	RMS(x)	0.28	0.27	2.5%	0.26	5.5%	0.21	26.4%
	Peak(y)	3.35	2.75	17.9%	2.82	15.9%	2.76	17.6%
	RMS(y)	0.55	0.46	15.7%	0.40	26.9%	0.41	26.4%
El Centro (0.2 g)	Peak(x)	2.49	2.05	17.7%	1.67	33.0%	1.78	28.3%
	RMS(x)	0.41	0.45	-9.3%	0.40	0.8%	0.31	24.5%
	Peak(y)	6.46	4.46	30.9%	3.52	45.5%	4.58	29.1%
	RMS(y)	0.83	0.60	27.0%	0.53	36.1%	0.55	33.3%
Wenchuan (0.1 g)	Peak(x)	2.33	2.27	2.5%	1.40	40.0%	2.48	-6.3%
	RMS(x)	0.46	0.46	-1.3%	0.33	27.5%	0.42	8.1%
	Peak(y)	5.33	5.33	0.1%	2.53	52.5%	5.11	4.2%
	RMS(y)	1.02	0.90	12.0%	0.56	45.1%	0.81	20.3%
Wenchuan (0.2 g)	Peak(x)	6.76	5.50	18.7%	3.52	47.9%	3.67	45.6%
	RMS(x)	1.22	1.34	-9.9%	0.78	36.0%	0.78	36.1%
	Peak(y)	2.37	2.47	-3.9%	1.38	41.8%	1.70	28.3%
	RMS(y)	0.37	0.48	-28.1%	0.30	19.8%	0.29	22.2%

single PTMD against two-dimensional earthquake might not be the best solution. Multiple PTMDs may solve this issue and the test will be conducted in the future study.

6. Conclusions

PTMD can make use of the energy dissipated during impact and is believed to have better ability on reducing the earthquake responses of the host structure over traditional TMD. The efficacy of the PTMD in reducing the structural responses for a wide range of earthquake loading conditions has been demonstrated in a series of experiments conducted in the lab of Fuzhou University, China. In these experiments, the PTMD was adopted to control the responses of a frame structure. The uncontrolled, TMD and PTMD controlled situations were compared under different earthquake inputs.

• TMD exerts poor control effectiveness under earthquake inputs, sometimes it may even enlarge the responses of the host structure. In most cases, the PTMD was proved to perform significantly better than the traditional TMD, the improvement in both peak acceleration and RMS responses were remarkable. Under single dimensional earthquake, the optimal control effectiveness on the peak and the RMS responses can stay above 40% under different earthquake loading conditions.

• The initial gap is found to have great influence on the control effectiveness of the PTMDs. Excessive gap value will significantly decrease the control effectiveness. Moreover, the optimal selection of the initial gap value is realized to have strong connection with the input intensity. Note that although the performance of the PTMD controlled systems are much better than the TMD controlled systems

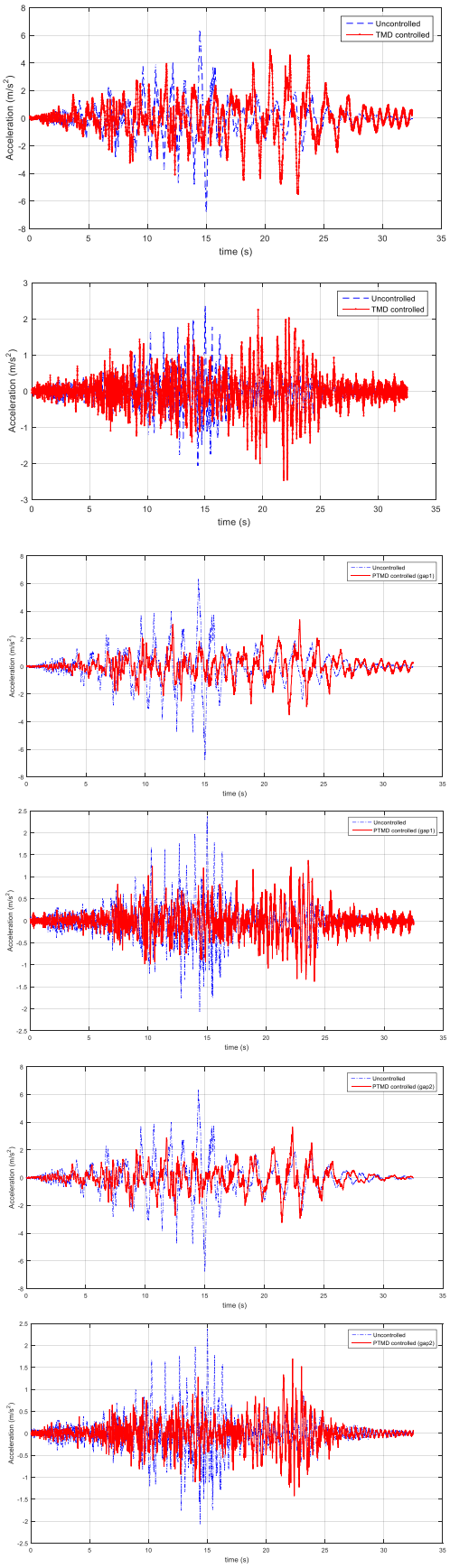

Fig. 10 Comparison of the time-history of the acceleration under two-dimensional Wenchuan earthquake (Left: acceleration along x-direction; Right: acceleration along y-direction)

during two-dimensional earthquake inputs, the control effectiveness seems to be unstable.

• Problems were found that an undesirable spiral vibration may occurs and the torsional vibration modes may be generated if using single PTMD against two-dimensional earthquake inputs. Efforts are currently under way to investigate the optimal design on PTMD parameters, to further validate the robustness of the PTMD and the experimental study on the application of multiple PTMDs.

Acknowledgments

The authors are grateful for financial support by National Natural Science Foundation of China (no. 51578159, no. 51678158), Program for New Century Excellent Talents in Fujian Province University (no. 83016017), Co-operative project in Fujian province colleges and universities (no. 2016H6011) and Co-operative leading project in Fujian province colleges and universities (no. 2017H0016).

References

Casado, C.M., Poncela, A.V. and Lorenzana, A. (2007), "Adaptive tuned mass damper for the construction of concrete piers", *Struct. Eng.*, **17**(3), 252-255.

Chen, S.H., Lin, W., Yu, J.X. and Qi, A. (2014), "Free-interface modal synthesis based substructural damage detection method", *Shock Vibr.*

Eason, R.P., Sun, C., Dick, A.J. and Nagarajaiah, S. (2013), "Attenuation of a linear oscillator using a nonlinear and a semi-active tuned mass damper in series", *J. Sound Vibr.*, **332**(1), 154-166.

Inaudi, J.A. and Kelly, J.M. (1995), "Mass damper using friction-dissipating devices", *J. Eng. Mech.*, **121**(1), 142-149.

Kawaguchi, A., Teramura, A. and Omote, Y. (1992), "Time history response of a tall building with a tuned mass damper under wind force", *J. Wind Eng. Industr. Aerodyn.*, **43**(1), 1949-1960.

Lee, C.L., Chen, Y.T., Chung, L.L. and Wang, Y.P. (2006), "Optimal design theories and applications of tuned mass dampers", *Eng. Struct.*, **28**(1), 43-53.

Li, H.N., Yi, T.H., Ming, G.U. and Huo, L.S. (2009), "Evaluation of earthquake-induced structural damages by wavelet transform", *Progr. Nat. Sci.*, **19**(4), 461-470.

Li, J. and Hao, H. (2016), "A review of recent research advances on structural health monitoring in Western Australia", *Struct. Monitor. Mainten.*, **3**(1), 33-49.

Lin, G.L., Lin, C.C., Chen, B.C. and Soong, T.T. (2015), "Vibration control performance of tuned mass dampers with resettable variable stiffness", *Eng. Struct.*, **83**, 187-197.

Lin, W., Chen, S.H., Yu, J.X. and Qi, A. (2013), "Seismic behavior of long-span connected structures under multi-supported and multi-dimensional earthquake excitations", *Adv. Struct. Eng.*, **16**(9), 1579-1586.

Lin, W., Lin, Y., Song, G. and Li, J. (2016), "Multiple pounding tuned mass damper (MPTMD) control on benchmark tower subjected to earthquake excitations", *Earthq. Struct.*, **11**(6), 1123-1141.

Lin, W., Song, G.B. and Chen, S.H. (2017), "PTMD control on a benchmark TV tower under earthquake and wind load excitations", *Appl. Sci.*, **7**(4), 7040425.

Lu, X., Zhang, Q., Weng, D., Zhou, Z., Wang, S., Mahin, S.A. and Qian, F. (2017), "Improving performance of a super tall building using a new eddy-current tuned mass damper", *Struct. Contr. Health Monitor.*, **24**(3).

Nagarajaiah, S. (2009), "Adaptive passive, semiactive, smart tuned mass dampers: identification and control using empirical mode decomposition, hilbert transform, and short-term fourier transform", *Struct. Contr. Health Monitor.*, **16**(7-8), 800-841.

Occhiuzzi, A., Spizzuoco, M. and Ricciardelli, F. (2008), "Loading models and response control of footbridges excited by running pedestrians", *Struct. Contr. Health Monitor.*, **15**(3), 349-368.

Ricciardelli, F., Occhiuzzi, A. and Clemente, P. (2000), "Semi-active tuned mass damper control strategy for wind-excited structures", *J. Wind Eng. Industr. Aerodyn.*, **88**(1), 57-74.

Roberto, V. (1994), "Seismic control of structures with resonant appendages", *Proceedings of the 1st World Conference on Structural Control*, Los Angeles, California, U.S.A.

Roberto, V. and Scott, C.M. (1995), "Passive seismic control of cable-stayed bridges with damped resonant appendages", *Earthq. Eng. Struct. Dyn.*, **24**(2), 233-246.

Song, G.B., Zhang, P., Li, L.Y., Singla, M., Patil, D., Li, H.N. and Mo, Y.L. (2016), "Vibration control of a pipeline structure using pounding tuned mass damper", *J. Eng. Mech.*, **142**(6), 04016031.

Soong, T.T. and Spencer Jr, B.F. (2002), "Supplemental energy dissipation: State-of-the-art and state-of-the-practice", *Eng. Struct.*, **24**(3), 243-259.

Tubino, F. and Piccardo, G. (2015), "Tuned mass damper optimization for the mitigation of human-induced vibrations of pedestrian bridges", *Meccan.*, **50**(3), 809-824.

Varadarajan, N. and Nagarajaiah, S. (2004), "Wind response control of building with variable stiffness tuned mass damper using empirical mode decomposition/hilbert transform", *J. Eng. Mech.*, **130**(4), 451-458.

Weber, B. and Feltrin, G. (2010), "Assessment of long-term behavior of tuned mass dampers by system identification", *Eng. Struct.*, **32**(11), 3670-3682.

Weber, F., Distl, H., Fischer, S. and Braun, C. (2016), "MR damper controlled vibration absorber for enhanced mitigation of harmonic vibrations", *Appl. Sci.*, **5**(4), 5040027.

Xiang, P. and Nishitani, A. (2014), "Seismic vibration control of building structures with multiple tuned mass damper floors integrated", *Earthq. Eng. Struct. Dyn.*, **43**(6), 909-925.

Xu, Y.L., Samali, B. and Kwok, K.C.S. (1992), "Control of along-wind response of structures by mass and liquid dampers", *J. Eng. Mech.*, **118**(1), 20-39.

Yi, T.H., Li, H.N. and Sun H.M. (2013), "Multi-stage structural damage diagnosis method based on "energy-damage" theory", *Smart Struct. Syst.*, **12**(3-4), 345-361.

Yi, T.H., Li, H.N. and Zhang, X.D. (2015), "Health monitoring sensor placement optimization for canton tower using immune monkey algorithm", *Struct. Contr. Health Monitor.*, **22**(1), 123-138.

Zhang, P., Song, G., Li, H.N. and Lin, Y.X. (2012), "Seismic control of power transmission tower using pounding TMD", *J. Eng. Mech.*, **139**(10), 1395-1406.

Zhang, Z. and Ou, J.P. (2017), "Optimization design of coupling beam metal damper in shear wall structures", *Appl. Sci.*, **7**(2), 7020137.

HK